AIAA 81-0334R

Scaling of Two- and Three-Dimensional Shock/Turbulent Boundary-Layer Interactions at Compression Corners

Gary S. Settles* and Seymour M. Bogdonoff†
Princeton University, Princeton, N.J.

This paper begins by considering how the upstream influence of a two-dimensional shock wave/turbulent boundary-layer interaction scales with the parameters of the incoming flow. Several recent experiments with equilibrium, supersonic, adiabatic turbulent boundary layers are considered in this light. Based on dimensional analysis, a functional relation is found among the upstream influence and the related parameters δ_0, Re, α, and M_∞. Then, an explicit correlation of these parameters is derived from the experimental data. The correlation demonstrates that, when upstream influence is scaled by boundary-layer thickness, an $Re_{\delta 0}$ "residual" remains. Further, some long-standing discrepancies among the experiments in this field are largely accounted for. Then, the upstream influence of three-dimensional interactions is examined to see if it scales in a manner similar to that of two-dimensional interactions. Based on measurements presented here for the first time, this is indeed the case, with the important provision that the flow development in both the streamwise and spanwise directions must be scaled simultaneously.

Nomenclature

a,b,c,d = powers used in dimensional analysis
c_f = skin friction coefficient
c_{f0}^* = correlation intercept parameter (Ref. 22)
L_m = upstream influence distance, cm (see Fig. 2)
M = Mach number
p = pressure, N/m^2
Re = freestream Reynolds number, u_∞/ν_∞, m^{-1}
Re_δ = Reynolds number based on boundary-layer thickness
u = velocity, m/s
x = distance along test surface in freestream direction, cm
y = distance above and normal to test surface, cm
z = spanwise distance normal to x axis, measured from left edge of corner model, cm
α = compression corner angle measured in x-y plane, deg
δ = boundary-layer thickness, cm
δ_ℓ = local incoming boundary layer thickness just upstream of three-dimensional interaction, cm
λ = compression corner sweepback angle measured in x-z plane, deg
ν = kinematic viscosity, m^2/s
σ = upstream influence coefficient (Ref. 22)

Subscripts

0 = undisturbed conditions at corner location in the absence of an interaction
∞ = freestream conditions

Introduction

We consider here the problem of a shock wave interacting with a turbulent boundary layer, which holds importance in modern fluid mechanics because of its practical significance and its level of difficulty. The practical significance is found in many areas of air transportation and fluid machinery, while the difficulty arises from the nonlinear combination of such complex elements as compressibility, self-induced viscous-inviscid interaction, flow separation, and of course, turbulence. While the Navier-Stokes equations governing this phenomenon are known, their direct and routine solution is well beyond the current state-of-the-art. So, even in an era of major advances in computational fluid mechanics, the shock wave/turbulent boundary-layer interaction remains rooted in experimental ground.

Several recent reviews[1-4] have discussed these matters in detail. From them, and from an extensive background of past studies, one sees that future progress in the understanding and prediction of these interactions hinges on some key issues for which the present fund of knowledge is inadequate. At the most fundamental level, the mechanics of turbulence is not known, and there are insufficient empirical data on which to base a proper model of turbulence in a shock/boundary-layer interaction. At a more practical level, even the overall scaling laws of interaction size, shape, and character are largely unknown, so that those methods of analysis and correlation less sophisticated than Navier-Stokes solutions still must be based on inadequate observations. There is clearly a need for further experimental work over ranges of fluid and geometrical parameters in order to discover the nature of shock/boundary-layer interaction scaling laws.

In this paper we are concerned specifically with the scaling of the upstream influence of compression corners on flat surfaces with incoming supersonic turbulent boundary layers. There are several reasons for this choice. Regardless of geometry, the upstream influence is a primary interaction characteristic which one needs to understand and predict, and it is relatively easy to measure accurately. The compression corner geometry lends itself well to this purpose because it allows reasonably interference-free flows, provides a positive corner-line reference for upstream influence measurements, and has practical aerodynamic applications in flares, control surfaces, inlets, etc.

For flow conditions, the equilibrium turbulent boundary layer at moderate to high Reynolds numbers is chosen as a well-defined incoming boundary condition for the interaction, which also simulates full-scale flight conditions directly. Finally, a supersonic freestream is chosen because of the relative simplification of an external hyperbolic flow.

The present study is an extension of earlier work by the authors[5-7] on both two-dimensional (2D) and three-

Presented as Paper 81-0334 at the AIAA 19th Aerospace Sciences Meeting, St. Louis, Mo., Jan. 12-15, 1981; submitted Feb. 23, 1981; revision received Oct. 15, 1981.

*Research Staff Member and Lecturer, Gas Dynamics Laboratory, Mechanical and Aerospace Engineering Department. Member AIAA.

†Professor and Chairman, Mechanical and Aerospace Engineering Department. Fellow AIAA.

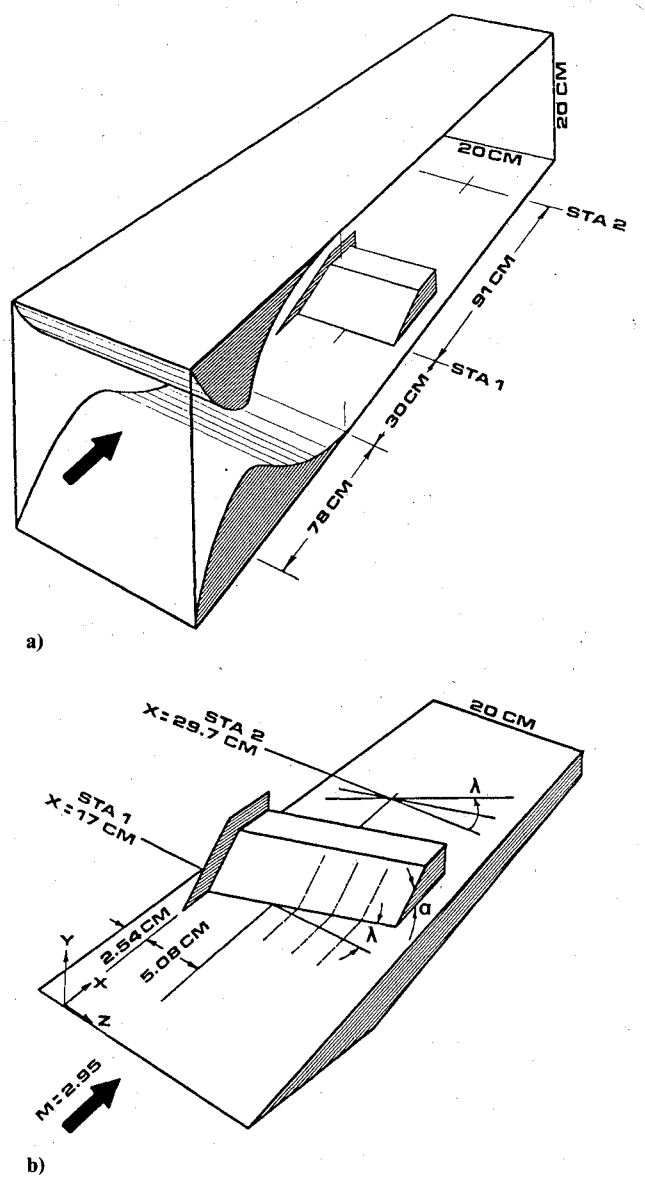

Fig. 1 a) Princeton high Reynolds number supersonic tunnel and b) flat plate test model with swept corner.

dimensional (3D) compression corner flows. The earlier 2D work considered Reynolds number scaling and incipient separation, while the first phase of the 3D investigation[6] sought to gain some basic knowledge in an area which had not been explored before in detail. Major questions arose[6] about the scaling laws for 3D interactions in general, and about Reynolds number scaling in particular. In a continuing research program which includes the present work, we are attempting to answer these questions through experiments over wide ranges of freestream Reynolds number Re and boundary layer thickness δ. However, it has become clear that the 3D scaling problem cannot be treated adequately without first reconsidering the limiting 2D case in detail, since the 2D Reynolds number scaling of upstream influence was not well defined in the literature.

Green[1] recognized this problem in 1970, stating that the available 2D experiments showed too great a disparity to serve as the basis of a correlation. In ten years this situation has changed somewhat with the advent of new experiments. In particular, there are now at least three high-quality data sets available[7-9] on the Reynolds number scaling of compression corner interactions for the same nominal flow conditions (equilibrium, adiabatic turbulent boundary layers at $M \sim 3$).

The present work begins with a fresh look at 2D upstream influence scaling in the light of these recent experiments. Having reconciled the 2D experimental disparities noted by Green, at least over a limited range of flow conditions, we then proceed to consider the 3D scaling problem. The second phase of the experimental program begun in Ref. 6 is introduced, and some conclusions are drawn about Reynolds number scaling in swept corner flows and how it relates to the 2D case.

Description of Experiments

The present review of 2D upstream influence scaling relies mainly on the published experimental results of Law,[9] Roshko and Thomke,[8] and Settles,[5,7] wherein detailed accounts of the individual experiments are given. An account of the initial 3D experiments of the present authors is found in Ref. 6. This section is thus kept appropriately brief.

In general the experiments all involve compression corners on adiabatic walls with incoming equilibrium turbulent boundary layers. A Reynolds number range of $10^5 \leq Re_{\delta 0} \leq 10^7$ is covered at a freestream Mach number of about 3. The Roshko-Thomke tests involved a blowdown wind tunnel with a 1.2-m test section. Law's tests and those of the present authors were done in separate but almost identical blowdown facilities with 20×20-cm test sections. The test geometries and dimensions of the Princeton high Reynolds number tunnel are shown in Fig. 1.

Summary of Test Conditions

Law's experiments were done at a single station 30.5 cm from the leading edge on a flat plate with $3.1 \times 10^7/\text{m} \leq Re \leq 31.0 \times 10^7/\text{m}$ and corner angles α between 15 and 26 deg. The Roshko-Thomke experiments were done at a single station 3.76 m downstream of the nozzle exit on their wind tunnel floor, with $1.6 \times 10^7/\text{m} \leq Re \leq 5.9 \times 10^7/\text{m}$ and $15 \leq \alpha \leq 25$ deg. The Princeton experiments were done at two stations 29.7 and 121 cm from the nozzle exit on the wind tunnel floor, and at two stations 17 and 29.7 cm from the leading edge of a flat plate. The unit Reynolds number range was identical to that of Law, but corner angles between 10 and 24 deg were tested. In none of the preceding experiments were all corner angles tested at all flow conditions.

In the swept compression corner experiments of Ref. 6, tests were done only at the two flat-plate stations and only at Re values of 6.3 and $18.7 \times 10^7/\text{m}$. Streamwise corner angles of 16 and 24 deg were tested over a range of sweepback angle λ, of 0-40 deg. The same streamwise corner angle was maintained at each value of λ.

In additional swept corner experiments reported here for the first time, another corner angle was added ($\alpha = 10$ deg) and the sweepback range was extended to $\lambda = 60$ deg for all three corner angles. The range of test conditions was also extended to include the first station on the wind tunnel wall. These extensive additions to the test program were required to explore the range of swept corner flows more fully, and to approach the scaling problem with two values of freestream Reynolds number and incoming boundary-layer thicknesses varying over a range of 6:1. While not all combinations were tested, 24 separate models were tested with a total of 56 combinations of α, λ, Re, and δ. Several measures and checks were taken to insure that the experiments were not compromised by end effects.[6]

Incoming Boundary Layers

The state of the incoming turbulent boundary layers in these experiments is of crucial importance if the results are to be considered reproducible, and thus in any way representative of standard test cases. (This is one reason to confine one's view to moderately high Reynolds numbers, since the literature reveals that results taken too near transition generally cannot be reconciled among themselves.)

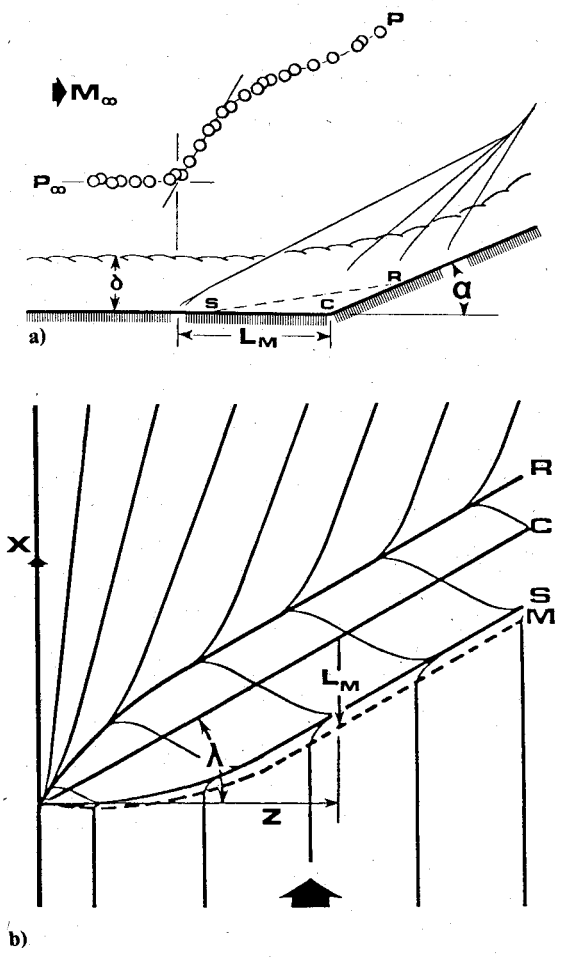

Fig. 2 Determination of upstream influence length a) from pressure distribution and b) from surface flow patterns; C≡corner, M≡maximum upstream influence, R≡reattachment, and S≡separation.

Law and Roshko and Thomke each have justified the condition of their boundary layers in their respective publications. In our experiments the compressible wall-wake similarity law[10,11] is used as a criterion with which to judge the condition of the incoming boundary layers. Across the range of test conditions, the boundary-layer mean-velocity profiles displayed a good fit to the wall-wake law with c_f values in agreement with the Van Driest II theory and values of the wake-strength parameter Π within the accepted range for equilibrium turbulent boundary layers. Some typical profiles are illustrated in the preprint version of this paper.[12]

Measurement Techniques

The important measurements in all the experiments considered here are surface pressure distributions and surface-streak or oil-flow patterns. These basic measurements are sufficient to determine the upstream influence length of flow about a compression corner (though they are not adequate to describe the related flowfield).

Figure 2a shows the method used in Refs. 7-9 to determine the upstream influence length from a surface pressure distribution. One strikes a line through the maximum slope of the distribution ahead of the corner, then takes the intersection of this line with the horizontal defined by $p=p_\infty$ to locate the upstream influence length L_m.

An equivalent technique is also used here and in Ref. 6; L_m is determined at the boundary between disturbed and undisturbed streak lines in the surface flow patterns (Fig. 2b). A kerosene-lampblack streak method is used (Ref. 7, Appendix B), which permits detailed, full-scale streak traces to be obtained. Extensive checks of the pressure distribution and surface flow methods in both 2D and 3D flows have shown that they are equivalent within the obtainable measurement accuracy.

Figure 2b also shows the coordinate system used for 3D upstream influence measurements, wherein L_m is measured in the streamwise direction as a function of the perpendicular spanwise dimension z. This system was chosen mainly for convenience; a corner-normal coordinate system might have been used as well, differing only by a geometrical transformation.

Two-Dimensional Upstream Influence Scaling

The basic question is: what is an appropriate scaling law for the upstream influence of 2D compression corner interactions? There is no simple answer to this question in the literature. Most investigators at least agree that an increase in α increases the scale while an increase in M_∞ decreases it. However, the effect of Reynolds number is a matter of controversy.[1]

The experiments of Chapman et al.[13] and those of Kuehn[14,15] demonstrated that the upstream influence, when scaled by boundary-layer thickness, increased with an increase in Reynolds number. For years these were the definitive experiments on shock-induced separation, even though they were conducted at low turbulent Reynolds numbers with tripped boundary layers. Hammitt and Hight[16] were among the first to demonstrate a reversal of this trend at higher Reynolds numbers, followed by Roshko and Thomke[8] and others.[5,7,9] In fact, the high Reynolds number trend of decreasing upstream influence with increasing Reynolds number has now been demonstrated from transonic[17,18] to hypersonic[19] Mach numbers.

There may be good reason to believe that a reversal of the Reynolds number effect occurs somewhere downstream of transition.[20] Elfstrom[21] has given a plausible explanation based on the development of the wake component of the turbulent boundary layer after transition. In any case, we have avoided this problem by confining attention to Re_δ above about 10^5, where all investigators agree that the inverse relationship holds and where most of the practical applications lie.

Dimensional Analysis

According to Green,[1] "In two-dimensional flow the length of a separation bubble should depend on: the magnitude of the overall pressure rise, the nature of the disturbance which causes it, the Mach number and Reynolds number of the initial flow, and some measure of the thickness of the undisturbed boundary layer." If one accepts that these are all of the variables, then a simple dimensional analysis should reveal the form of the interaction scale.

If we restrict attention solely to compression corners, then Green's first two parameters reduce simply to the corner angle α. However, there is still the question of which thickness and which Reynolds number to choose. Following Green, we choose δ_0 for the thickness; it is simple, commonly reported, and essentially linear with the integral thicknesses, δ^* and θ, for present purposes. For the Reynolds number one could choose either $Re_{\delta 0}$ or Re_x, bearing in mind that neither δ_0 nor x is independent of the previously chosen boundary-layer thickness scale. Since the virtual origin of a turbulent boundary layer is poorly defined, $Re_{\delta 0}$ is the preferable choice. The general result of the analysis is then

$$L_m/\delta_0 = f(Re_{\delta 0}, \alpha, M_\infty) \tag{1}$$

Alternatively, one could render all terms independent by expressing Reynolds number merely as $u_\infty/\nu_\infty\ (\equiv Re)$, which has the dimension of inverse length. In this case, dimensional consistency requires that we form a single nondimensional group from L_m, Re, and δ_0, to wit, $(L_m Re^{-a})/\delta_0^{a+1}$.

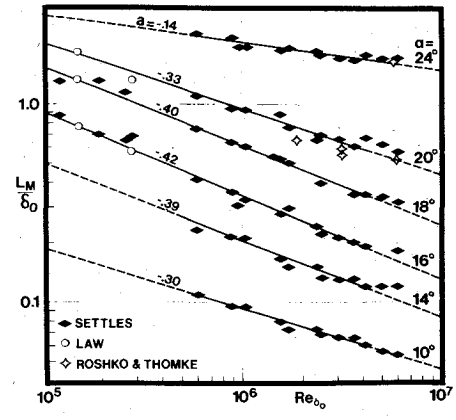

Fig. 3 Variation of upstream influence length with boundary-layer thickness and Reynolds number; determination of "a" values.

Equation (1) can then be rewritten as

$$(L_m Re^{-a})/\delta_0^{a+1} = (L_m/\delta_0) Re_{\delta_0}^{-a} = f(\alpha, M_\infty) \qquad (2)$$

It remains for the validity of this power-law relationship, the value of "a," and the forms of the α and M_∞ functions to be determined empirically.

Experimental Results

Drawing upon the previously-described experiments with $M_\infty \sim 3$ and ranges of α and Re_{δ_0}, we plot L_m/δ_0 vs Re_{δ_0} in Fig. 3 and seek to determine the nature of the power a. This figure illustrates that there is good agreement among the experiments of Law, Roshko and Thomke, and Settles. In each case the value of L_m/δ_0 declines weakly with increasing Re_{δ_0}. The power a varies from -0.30 at $\alpha = 10$ deg (attached flow) to -0.42 at $\alpha = 16$ deg (incipient separation), to -0.14 at $\alpha = 24$ deg (separated flow).

Strictly speaking, one should set $a = a(\alpha)$ in Eq. (2) for the scale of the interaction. We have not done so here because a is a weak function of α, and because we believe that considering it so is not warranted by the overall accuracy of the measurements. Instead, we have taken a simple average value from Fig. 3, $a = -1/3$, although it is important to recognize that $a = a(\alpha)$ may be necessary outside the range of present conditions.

With $a = -1/3$, Eq. (2) becomes

$$L_m Re^{1/3}/\delta_0^{2/3} = (L_m/\delta_0) Re_{\delta_0}^{1/3} = f(\alpha) \quad (M_\infty \sim 3) \qquad (3)$$

from which one sees that $L_m \sim \delta_0^{2/3}$ at fixed Re, while $L_m \sim Re^{-1/3}$ at fixed δ_0, with α and M_∞ held constant. These relations may not apply outside the ranges of α, Re_{δ_0}, and M_∞ considered here, and the powers shown are approximate in any case; but the message is clear: if the upstream influence length is scaled by δ_0, then an Re_{δ_0}, "residual" remains.

This scaling could be expressed in other forms as well, since δ_0^* or θ_0 could have been used instead of δ_0 to achieve substantially the same result. Also, since $c_f \sim Re_{\delta_0}^{-1/6}$ (at least for the Princeton experiments), one could write $L_m/\delta_0 \sim c_{f_0}^2$ to the same level of accuracy.

The L_m/δ_0 dependence on Re_{δ_0} has been recognized in some earlier publications[16-20,22] including those of the present authors.[5,7,23] Hammitt and Hight, in fact, found limited empirical support for the $-1/3$ power dependence noted here.

Correlations and Predictions

Given Eq. (3), a logical next step is to find the form of the α-scaling function. A graphical analysis of the data shows that an exponential function works quite well over the range of conditions covered here. Accordingly, the data of Fig. 3 are shown again in Fig. 4 in terms of $(L_m/\delta_0) Re_{\delta_0}^{1/3}$ vs α in semilogarithmic coordinates. The data of Law, Roshko and Thomke, and Settles are reasonably correlated by the simple formula

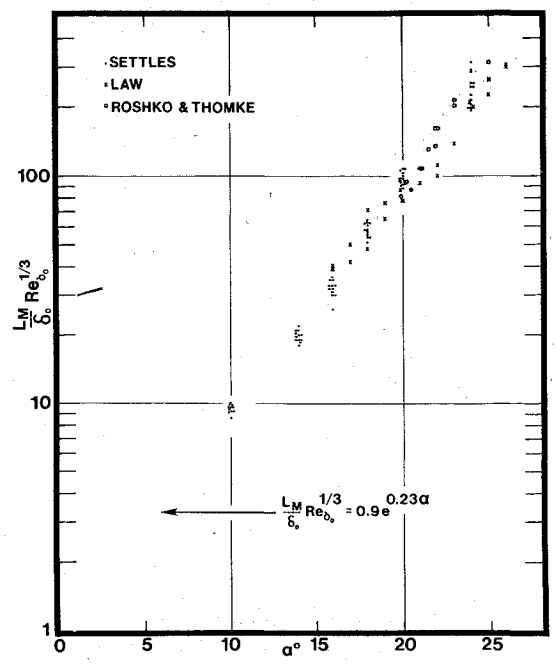

Fig. 4 2D compression corner upstream influence correlation; $M \sim 3$, $10^5 \le Re_{\delta_0} \le 10^7$, 10 deg $\le \alpha \le$ 26 deg.

$$(L_m/\delta_0) Re_{\delta_0}^{1/3} = 0.9e^{0.23\alpha} \quad (M_\infty \sim 3) \qquad (4)$$

(A similar result was mentioned in Refs. 6 and 7, but the formula was printed incorrectly.)

The spread of the data about Eq. (4) is worst at the highest α, as expected, where it amounts to $\pm 25\%$. The correlation could be improved at the expense of greater complexity by considering $a = a(\alpha)$, but this has not been done in view of the experimental difficulties which limit the overall accuracy of the data. These difficulties include the inherent inaccuracy in determining L_m and δ_0, possible Re variations during experiments, differences of unknown character between experimental facilities, possible 3D perturbations of 2D experiments, and—in a few cases—the difficulty of extracting the desired quantities from published literature.

Having arrived at the correlation of Eq. (4), we now compare it with another correlation for compression corner upstream influence due to Roshko and Thomke.[22] Their correlation was based on an additional set of experiments they conducted using an axisymmetric "stove-pipe" body. They found that plotting L_m/δ_0 vs c_{f_0} correlated not only Re and δ_0 variations, but M_∞ variations as well. The resulting correlation equation was

$$L_m/\delta_0 = \sigma(\alpha)\,[c_{f_0} - c_{f_0}^*(\alpha)] \qquad (5)$$

For comparison with present results we have used Roshko and Thomke's stated formulas for $\delta(Re,x)$ and $\theta(Re,x)$ along with $c_f \cong 2\mathrm{d}\theta/\mathrm{d}x$ to arrive at $c_{f_0} \sim Re_{\delta_0}^{-1/7}$ at $M \sim 3$ for their experiments. Using this in Eq. (5) with α fixed results in $L_m/\delta_0 \sim Re_\delta^{-1/7}$, which is the same functional form as Eqs. (3) and (4), but with a different power. With these substitutions, a comparison between Eqs.(4) and (5) is illustrated in Fig. 5.

The two correlations agree within the data scatter for α less than about 20 deg. Above 20 deg the Roshko-Thomke correlation deviates systematically below the present results. We believe that there is a simple explanation for this, since the axisymmetric results of Roshko and Thomke would not be

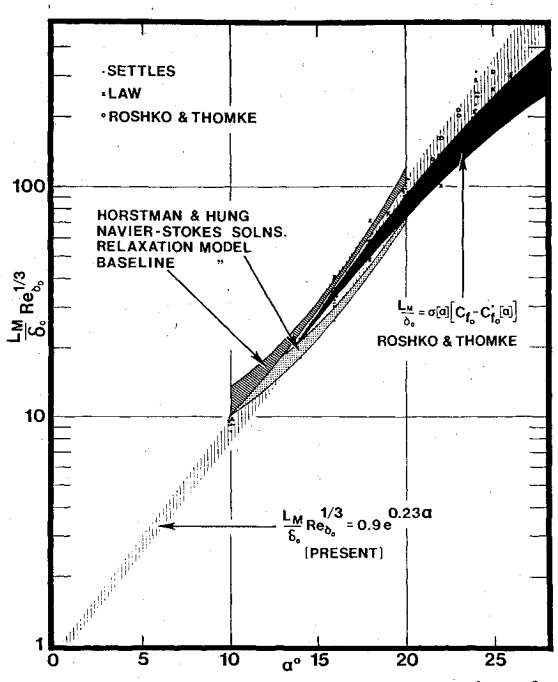

Fig. 5 Comparison of correlations and computations for 2D compression corner upstream influence.

expected to reproduce 2D results for sizeable separated regions, where transverse curvature comes into play. We have seen similar effects in our own axisymmetric experiments.[5,7] This discrepancy arises from the empirical function $\sigma(\alpha)$ in Eq. (5), not from the inherent $Re_{\delta 0}$ dependence of c_{f0}.

Also shown in Fig. 5 are the results of numerical solutions of the Navier-Stokes equations by Horstman and Hung,[23] wherein an algebraic eddy viscosity (baseline) model and a modified relaxation eddy viscosity model were used for turbulence closure. These results are also in general agreement with the correlations except near $\alpha = 10$ deg. It is interesting to see that the Navier-Stokes solutions essentially confirm the $Re_{\delta 0}^{1/3}$ scaling of upstream influence lengths found here, though one must bear in mind that the present state-of-the-art of Navier-Stokes solutions with turbulence modeling is scarcely to be trusted any more than empirical correlations. (See, for example, Refs. 23 and 24 for illustrations of the inadequacy of the computations for predicting separated flows.)

In summary, discrepancies among the various experiments on 2D shock wave/turbulent boundary-layer interactions have been noted by reviewers[1,2] and by the experimenters themselves.[5,9,16,22] We believe some progress is shown here in resolving these discrepancies, at least for the rather limited ranges of α, $Re_{\delta 0}$, and M_∞ that we have examined.

Three-Dimensional Upstream Influence Scaling

Compared with the situation for 2D interactions, any discussion of 3D upstream influence scaling must begin with a meager background of experimental evidence. There have been a few notable publications[6,25-29] beginning with Stalker,[30,31] but no one has made the concentrated effort nor had the fund of evidence required to make a definitive statement on the subject. In what follows, we present a first step in this process.

Dimensional Analysis

Beginning with the background developed earlier for 2D interactions, we rewrite Eq. (1) with two additional variables describing 3D interactions, namely, the sweepback angle λ and the spanwise dimension z

$$L_m = f(Re, \delta, z, \alpha, \lambda, M_\infty) \tag{6}$$

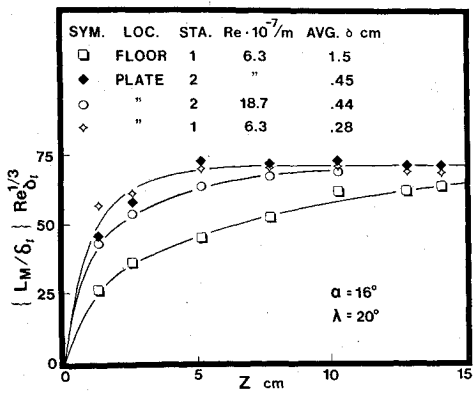

Fig. 6 Streamwise scaling of upstream influence for a swept compression corner case at $M_\infty \sim 3$.

Holding the dimensionless variables α, λ, and M_∞ constant for the present, we are left with Re, δ, and z involving only the length dimension. We expect the 3D upstream influence to depend upon two parameters which are combinations of these three variables. For dimensional consistency, one parameter must have length dimensions while the other must be dimensionless.

Consider the limit as $\lambda \to 0$. Scaling by λ and z becomes degenerate in this case and we expect to recover the 2D scaling in the form of Eq. (2). Thus one of the 3D parameters (the one with length dimensions) must be $Re^a \delta^{a+1}$ as before, and it must combine with L_m to form the general dimensionless streamwise scaling parameter $(L_m Re^{-a})/\delta^{a+1}$ for both 2D and 3D flows.

We are left with a single dimensionless parameter of the form $Re^b \delta^c z^d$ to describe the spanwise scaling of upstream influence for swept compression corners. Since z is the primary spanwise variable we choose $d = 1$, yielding a parameter of the form $z\,Re^{-b}/\delta^{b+1}$, which is analogous to the dimensionless streamwise scaling parameter $L_m Re^{-a}/\delta^{a+1}$. The complete functional form of the 3D upstream influence scaling can now be written as

$$\frac{L_m Re^{-a}}{\delta^{a+1}} = f\left(\frac{zRe^{-b}}{\delta^{b+1}}, \alpha, \lambda, M_\infty\right) \tag{7}$$

or, equivalently,

$$(L_m/\delta) Re_\delta^{-a} = f[(z/\delta) Re_\delta^{-b}, \alpha, \lambda, M_\infty] \tag{8}$$

Determining the nature of the scaling functions for α, λ, and M_∞ is beyond the scope of this paper. However, a and b can be found for limited flow conditions from the present experimental data.

Experimental Results

Given the requirement that Eqs. (7) and (8) must reduce to Eq. (2) in the limit as $\lambda \to 0$, one might expect to find the same empirical value of the power a for streamwise scaling in both 2D and 3D flows, that is, about $-\frac{1}{3}$ for present flow conditions. That this is so is demonstrated in Fig. 6, where the nondimensional upstream influence parameter $(L_m/\delta_\ell) Re_{\delta_\ell}^{1/3}$ is plotted vs z for several of our swept corner experiments at $\alpha = 16$ deg, $\lambda = 20$ deg, $M_\infty = 2.95$, and ranges of Re and δ_ℓ. (The local incoming boundary-layer thickness δ_ℓ is used here instead of δ_0 for an important reason. In highly swept interactions the incoming boundary-layer thickness may vary as much as 50% with span. Normalizing by δ_ℓ is thought to remove this otherwise uncontrolled variation, or at least to minimize it.) These test conditions were chosen especially for this purpose because they resulted in the development of cylindrically symmetric ($\partial L_m/\partial z = 0$) flow about the corner

line for large values of z, allowing a direct and independent test of the streamwise scaling. Indeed, $a=-\frac{1}{3}$ is shown to be appropriate for this purpose in Fig. 6, correlating the upstream influence of all the test conditions shown once cylindrical symmetry has been reached.

We also see from Fig. 6 that spanwise Re_{δ_ℓ} scaling is required, as predicted in the previous section, to correlate the various "inception" lengths required in the z direction to attain cylindrical flow. It remains to determine b in Eqs. (7) and (8) which accomplishes this purpose.

Insofar as the empirical values a and b are related to the upstream propagation mechanism in some way, there is little reason to suspect that they will differ very much for streamwise or spanwise scaling. It then comes as no surprise that $b=-\frac{1}{3}$ is found effective in correlating the spanwise scales of the data in Fig. 6. Having tentatively found $a=b=-\frac{1}{3}$ from the data, we can write Eq. (8) in its final form for the present

$$(L_m/\delta_\ell)Re_{\delta_\ell}^{1/3}=f[(z/\delta_\ell)Re_{\delta_\ell}^{1/3},\alpha,\lambda,M_\infty] \tag{9}$$

We emphasize that *there is nothing universal about the* $-\frac{1}{3}$ *power used here.* It is an average value for a limited range of test conditions. In fact, even within this range a parametric study shows that any values within about $-0.3\le a,b\le -0.4$ are acceptable. The empirical constant is likely to be different outside our Reynolds number range or at a different Mach number, but we believe the 3D scaling principle [Eq. (8)] will remain valid under more general conditions.

Now Eqs. (8) and (9) are put to a rigorous test. An attempt has been made to scale the entire range of swept compression corner upstream influence results described earlier using this approach. The results are shown in Figs. 7a-c for $\alpha=10$, 16, and 24 deg, respectively. For ranges of $0\le\lambda\le 60$ deg, $6.3\times10^7/\text{m}\le Re\le 18.7\times10^7/\text{m}$, and 0.25 cm $\le\delta_\ell\le$ 1.5 cm, the upstream influence data are correlated in terms of Re and δ_ℓ within the accuracy of the measurements. Such a powerful correlation of the experimental data leaves little doubt about the validity of Eq. (9) for the present test conditions. Further, the same scaling law has been found effective for a different type of 3D interaction—beween a swept incident shock wave and a turbulent boundary layer—in separate work reported by Dolling and Bogdonoff.[32]

Discussion and Physical Interpretation

The new concept presented here is that of the spanwise scaling, for which we offer the following brief physical interpretation. Beginning with the 2D shock wave/turbulent boundary-layer interaction at a compression corner, there is no characteristic physical dimension imposed upon the flow by the body geometry (as there is, for example, by a forward-facing step). The length scales of the interaction must therefore depend mainly on the incoming flow characteristics. If the flow is truly two-dimensional, then the interaction develops only in the streamwise direction and scales only in that direction, and then only in terms dictated by the incoming flow and the corner angle.

Once three-dimensionality is introduced by sweeping back the corner, the interaction becomes a developing flow in both streamwise and spanwise directions. However, since no characteristic physical dimension was introduced during the sweepback process, there still remain only the flow characteristics and the corner angles (α and λ) to dictate the spanwise scale. For fixed values of α and λ, any change in the spanwise development of the interaction must be due entirely to a change in the incoming flow characteristics, and must derive its scale therefrom. This interpretation summarizes the development of Eqs. (6-9) and their empirical justification in Figs. 6 and 7.

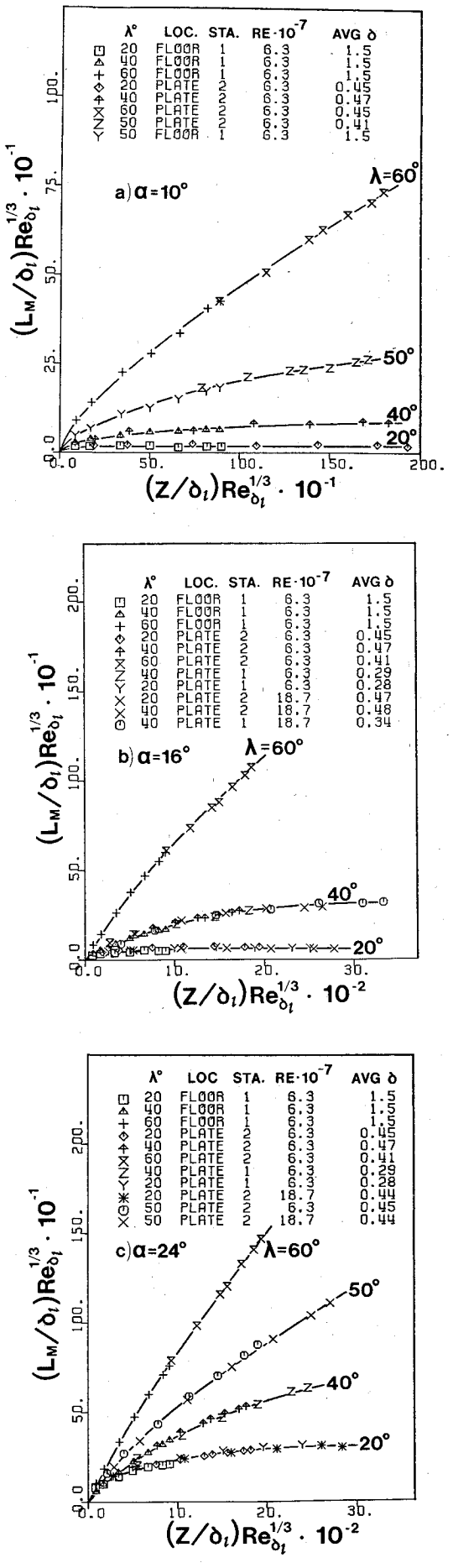

Fig. 7a-c Streamwise and spanwise scaling plots of upstream influence of swept compression corners at $M_\infty\sim3$, 10 deg $\le\alpha\le$ 24 deg.

Figures 7a-c represent in nondimensional terms the observed shapes of the upstream influence curves (illustrated by a dashed line in Fig. 2b) for a range of swept corner experiments. While the shape of each curve is fixed by the particular choice of α and λ, Eqs. (7-9) dictate that the dimensional scale can be compressed or expanded by changes in Re_{δ_ℓ}. For example, the spanwise distance required to establish cylindrical flow in Fig. 6 may be as small as 5 cm (for large Re and small δ_ℓ) or greater than 15 cm (small Re and large δ_ℓ).

This scaling principle has several practical applications. For example, it can be used to choose the optimum flow conditions under which to investigate 3D interactions in a wind tunnel of fixed dimensions (thin boundary layer at high Reynolds number if maximum coverage is desired). Further, given the dimensions of a 3D interaction region on a wind tunnel model, the interaction size at flight conditions could be estimated. While such applications are presently limited by the restricted nature of the empirical constants in the scaling law, continuing research should remove this obstacle in the future.

A further limitation arises from our lack of knowledge of the scaling functions for α, λ, and M_∞. Most of the flows represented by Fig. 7 exhibit significant regions of 3D separation which change character from cylindrically symmetric to conically symmetric as λ and α increase. The boundaries of this behavior and the scaling laws for each flow regime are subjects of our ongoing research program,[33] which also includes plans for experiments at a lower Mach number.

Summary and Conclusions

The latest phase of a research program on 2D and 3D shock wave/turbulent boundary-layer interactions is reported. Compression corner upstream influence scaling, particularly in terms of Reynolds number, is considered in the light of recent experiments at about Mach 3 with equilibrium turbulent boundary layers, adiabatic walls, and boundary-layer thickness Reynolds numbers between 10^5 and 10^7. The conclusions and observations are as follows.

1) For 2D interactions at fixed corner angle and Mach number, dimensional consistency requires that the scale of the interaction must be a ratio of freestream Reynolds number and boundary-layer thickness, both raised to fractional powers.

2) The 2D corner angle scaling is found to be exponential in form, leading to an upstream influence correlation for Mach 3 and high Reynolds numbers which is supported by the three leading experiments in that range.

3) A dimensional analysis of 3D interactions reveals that an additional nondimensional parameter is required to account for the spanwise scaling of the interaction development.

4) A correlation of new experimental data from swept compression corners reveals that the 3D scaling with Reynolds number in both the streamwise and spanwise directions is quantitatively similar to the streamwise scaling in 2D interactions.

5) Nondimensional curves are given for 3D upstream influence scaling as a function of corner and sweepback angles and Reynolds number over a range of incoming flow conditions.

6) The derived 3D scaling law reveals that the dimensional scale of an interaction can be compressed by decreasing boundary-layer thickness or increasing freestream Reynolds number, or can be expanded by converse measures.

Acknowledgments

Many of the 3D experiments reported here were performed by Jeffrey J. Perkins during his graduate study at Princeton. This work was supported by the U.S. Air Force Office of Scientific Research under Contracts F44620-75-C-0080 and F49620-80-C-0092, monitored by Dr. J. D. Wilson. Useful discussions with Drs. D. S. Dolling, G. R. Inger, and R. J. Stalker are gratefully acknowledged.

References

[1] Green, J. E., "Interactions Between Shock Waves and Boundary Layers," *Progress in Aerospace Sciences,* Vol. 11, 1970, pp. 235-340.

[2] Hankey, W. L. Jr. and Holden, M. S., "Two-Dimensional Shock-Wave Boundary Layer Interactions in High Speed Flows," AGARDograph No. 203, 1975.

[3] Stanewsky, E., "Shock-Boundary Layer Interaction in Transonic and Supersonic Flow," Von Karman Institute VKI-LS-59, 1973.

[4] Adamson, T. C. Jr. and Messiter, A. F., "Analysis of Two-Dimensional Interactions Between Shock Waves and Boundary Layers," *Annual Review of Fluid Mechanics,* Vol. 12, 1980, pp. 103-138.

[5] Settles, G. S., Bogdonoff, S. M., and Vas, I.E., "Incipient Separation of a Supersonic Turbulent Boundary Layer at High Reynolds Numbers," *AIAA Journal,* Vol. 14, Jan. 1976, pp. 50-56.

[6] Settles, G. S., Perkins, J. J., and Bogdonoff, S. M., "Investigation of Three-Dimensional Shock/Boundary-Layer Interactions at Swept Compression Corners," *AIAA Journal,* Vol. 18, July 1980, pp. 779-785.

[7] Settles, G. S., "An Experimental Study of Compressible Turbulent Boundary Layer Separation at High Reynolds Number," Ph.D. Dissertation, Aerospace and Mechanical Sciences Dept., Princeton University, Princeton, N. J., Sept. 1975.

[8] Roshko, A. and Thomke, G.J., "Supersonic, Turbulent Boundary Layer Interactions with a Compression Corner at Very High Reynolds Number," *Proceedings of the Symposium on Viscous Interaction Phenomena in Supersonic and Hypersonic Flow*, USAF Aerospace Research Labs, Wright-Patterson AFB, 1969, pp. 109-138.

[9] Law, C. H., "Two-Dimensional Compression Corner and Planar Sock Wave Interactions with a Supersonic, Turbulent Boundary Layer," ARL TR 75-0157, June 1975.

[10] Rotta, J. C., "Turbulent Boundary Layers with Heat Transfer in Compressible Flow," Report 60-02, Aerodynamische Versuchsanstalt Göttingen, Germany, Feb. 1960.

[11] Sun, C. C. and Childs, M. E., "A Modified Wall Wake Velocity Profile for Turbulent Compressible Boundary Layers," *Journal of Aircraft,* Vol. 10, June 1973, pp. 381-383.

[12] Settles, G. S., Perkins, J. J., and Bogdonoff, S. M., "Upstream Influence Scaling of 2D and 3D Shock/Turbulent Boundary Layer Interactions at Compression Corners," AIAA Paper 81-0334, Jan. 1981.

[13] Chapman, D. R., Kuehn, D. M., and Larson, H. K., "Investigation of Separated Flows in Subsonic and Supersonic Streams with Emphasis on the Effects of Transition," NACA Rept. 1356, 1958.

[14] Kuehn, D. M., "Experimental Investigation of the Pressure Rise Required for the Incipient Separation of Turbulent Boundary Layers in Two-Dimensional Supersonic Flow," NASA Memo 1-21-59A, 1959.

[15] Kuehn, D. M., "Turbulent Boundary-Layer Separation Induced by Flares on Cylinders at Zero Angle of Attack," NASA TR R-117, 1961.

[16] Hammitt, A. G. and Hight, S., "Scale Effects in Turbulent Shock Wave Boundary Layer Interactions," *Proceedings of the 6th Midwestern Conference on Fluid Mechanics,* AFOSR TN 60-82, Sept. 1959, pp. 362-382.

[17] Vidal, R. J., Wittliff, C. E., Catlin, P. A., and Sheen, B. H., "Reynolds Number Effects on the Shock Wave-Turbulent Boundary-Layer Interaction at Transonic Speeds," AIAA Paper 73-661, July 1973.

[18] Stanewsky, E. and Little, B. H., "Separation and Reattachment in Transonic Airfoil Flow," *Journal of Aircraft,* Vol. 8, Dec, 1971, pp. 952-958.

[19] Holden, M. S., "Shock Wave-Turbulent Boundary Layer Interaction in High Speed Flow," USAF ARL-TR-75-0204, June 1975.

[20] Green, J. E., "Some Aspects of Viscous-Inviscid Interactions at Transonic Speeds and their Dependence on Reynolds Number," AGARD-CP-83-71, Paper 2, 1971.

[21] Elfstrom, G. M., "Turbulent Separation in Hypersonic Flow," Imperial College Aero Rept. 71-16, 1971.

[22] Roshko, A. and Thomke, G. J., "Flare Induced Interaction Lengths in Supersonic, Turbulent Boundary Layers," *AIAA Journal*, Vol. 15, July 1976, pp. 873-879.

[23] Horstman, C. C., Settles, G. S., Vas, I. E., Bogdonoff, S. M., and Hung, C. M., "Reynolds Number Effects on Shock-Wave Turbulent Boundary Layer Interactions," *AIAA Journal*, Vol. 15, Aug. 1977, pp. 1152-1158.

[24] Settles, G. S., Fitzpatrick, T. J., and Bogdonoff, S. M., "Detailed Study of Attached and Separated Compression Corner Flowfields in High Reynolds Number Supersonic Flow," *AIAA Journal*, Vol. 17, June 1979, pp. 579-585.

[25] Avduyevskiy, V. S. and Gretsov, V. K., "Investigation of a Three-Dimensional Separated Flow Around Semicones Placed on a Plane Plate," NASA Tech. Trans. F-13, 578, 1971.

[26] Bachalo, W. D., "Three-Dimensional Boundary Layer Separation in Supersonic Flow," Univ. of California Berkeley, Rept. FM-74-10, Aug. 1974.

[27] Horstman, C. C. and Hung, C. M., 'Computation of Three-Dimensional Turbulent Separated Flows at Supersonic Speeds," AIAA Paper 79-2, Jan. 1979.

[28] Zheltovodov, A. A., "Properties of Two- and Three-Dimensional Separation Flows at Supersonic Velocities," Izvestiia Akademiia Nauk SSSR, *Mekhanika Zhidkosti i Gaza*, May-June 1979, pp. 42-50.

[29] Kussoy, M. I., Viegas, J. R., and Horstman, C. C., "An Experimental and Numerical Investigation of a 3D Shock Separated Turbulent Boundary Layer," AIAA Paper 80-0002, Jan. 1980.

[30] Stalker, R. J., "Sweepback Effects in Turbulent Boundary-Layer Shock-Wave Interaction," *Journal of the Aeronautical Sciences*, Vol. 27, May 1960, pp. 348-356.

[31] Stalker, R. J., "Viscous Effects in Supersonic Flow," Ph.D. Dissertation, Dept. of Aeronautics, Univ. of Sydney, Sydney, Australia, 1959.

[32] Dolling, D. S. and Bogdonoff, S. M., "Scaling of Blunt and Sharp Fin-Induced Shock Wave Turbulent Boundary Layer Interactions," AIAA Paper 81-0336, Jan. 1981.

[33] Ten, H.-Y. and Settles, G. S., "Cylindrical and Conical Upstream Influence Regimes of 3D Shock/Turbulent Boundary Layer Interactions," AIAA Paper 82-0987, June 1982.